Spin states and phase separation in $La_{1-x}Sr_xCoO_3$ ($x=0.15,0.25,0.35$) films: Optical, magneto-optical, and magnetotransport studies

N. N. Loshkareva,[1] E. A. Gan'shina,[2] B. I. Belevtsev,[3,*] Yu. P. Sukhorukov,[1] E. V. Mostovshchikova,[1] A. N. Vinogradov,[2] V. B. Krasovitsky,[3] and I. N. Chukanova[4]

[1]*Institute of Metal Physics of Ural Division of RAS, Ekaterinburg, 620219, Russia*

[2]*Moscow State University, Moscow, 119899, Russia*

[3]*B. Verkin Institute for Low Temperature Physics and Engineering, National Academy of Sciences, Kharkov 61103, Ukraine*

[4]*Institute for Single Crystals, National Academy of Sciences, Kharkov 61001, Ukraine*

(Received 3 October 2002; revised manuscript received 28 February 2003; published 23 July 2003)

Optical absorption and transverse Kerr effect spectra, resistivity, and magnetoresistance of $La_{1-x}Sr_xCoO_3$ ($x=0.15,0.25,0.35$) films have been studied. The temperature dependences of the optical and magneto-optical properties of the films exhibit features which can be attributed to the transition of the Co^{3+} ions from the low-spin state ($S=0$) to the intermediate-spin state ($S=1$) and to orbital ordering of the Co^{3+} ions in the latter state. The evolution of the properties influenced by doping with Sr is interpreted on the basis of the phase separation model.

DOI: 10.1103/PhysRevB.68.024413 PACS number(s): 72.80.Ga, 78.66.−w, 78.20.Ls

I. INTRODUCTION

The discovery of the so-called colossal magnetoresistance in manganite films[1] has renewed an interest in other ferromagnetic perovskitelike compounds. These include $LaCoO_3$-based cobaltites which are in many ways similar to manganites and yet have some fundamental distinctions. At low temperatures, $LaCoO_3$ is a nonmagnetic insulator. In this state Co^{3+} ions are mainly in the low-spin (LS) state $(t_{2g}^6, S=0)^2$ because the crystal-field energy dominates slightly over the intraatomic Hund's energy.[2,3] However, as the temperature rises, the Co^{3+} ion state changes gradually from the LS state to the high-spin (HS) state $(t_{2g}^4 e_g^2, S=2)$ or to the intermediate-spin (IS) state $(t_{2g}^5 e_g^1, S=1)$. The latter scenario is supported by the theoretical calculations[3,4] and results of some experimental studies.[5–8] The problem of spin states of Co^{3+} ions in cobaltites is not settled to date and remains topical.

When $LaCoO_3$ is doped with Sr^{2+} ions, hole-rich regions appear in the hole-poor matrix.[9] The evolution of the magnetic properties as a function of Sr^{2+} concentration x and temperature is governed by the transition from the spin-glass-like to cluster-glass state or to the ferromagnetic (FM) metallic state.[10,11] The certain scatter in the estimates obtained by different authors[9–11] for the critical Sr^{2+} concentration at which long-range FM order sets in is accounted for by such factors as instability against the formation of clusters rich in Sr^{2+} and containing ions in the IS state, the dependence of the chemical heterogeneity upon the thermal history of the samples, and the degree of oxidation. The question is still discussed considerably whether clusters are generated by compositional inhomogeneities when, for example, the phases with $x=0.5$ and $x=0.2$ are present in $La_{0.85}Sr_{0.15}CoO_3$,[12] or appear due to electron phase separation.[13]

In this article, a study of the Kerr effect, optical absorption, and transport phenomena in $La_{1-x}Sr_xCoO_3$ ($x=0.15,0.25,0.35$) films is presented. The phase separation in films can be expected to be somewhat more complicated as compared with bulk materials since it could depend on strain induced by the film-substrate lattice mismatch. At the same time, films are suitable objects which can be investigated by traditional electric and magnetic techniques giving averaged characteristics of the (inhomogeneous) material and by optical methods permitting one to separate responses from conducting regions and the insulating matrix and to study the magnetic processes inside the conducting clusters. This combined approach was applied earlier to manganites:[14,15] the charge inhomogeneities were studied by the optical absorption technique while the magnetically inhomogeneous state was investigated using the magneto-optical (MO) method.

Transport and optical properties of FM oxides are known to depend significantly on their magnetic properties. As for the MO properties, they are determined directly by the magnetization of a material studied. In this work, the MO properties were measured using the transverse Kerr effect (TKE). Generally, the MO Kerr effect consists in an influence of the magnetization of the medium on the reflected light. The TKE consists in the intensity variation of light reflected by a magnetized sample in conditions where the magnetic field is applied parallel to the sample surface and perpendicular to the light incidence plane. Measurements of MO spectra in the visible and near-ultraviolet spectral range—i.e., in the range of the fundamental absorption—could provide information concerning the electronic structure of the cobaltites and its dependence on chemical composition, conditions of the synthesis, and other factors. In particular, the appearance of the new type of magnetic ions, Co^{4+}, due to doping with Sr and/or change in the spin state of Co ions is expected to influence the MO spectra. The magnitude of the MO response is known to be the product of spin-orbit coupling strength and net electron spin polarization (magnetization). This makes the magneto-optical effects sensitive to the magnetic state of unfilled d shells in the transition-metal ions. MO spectroscopy provides not only information about the total density of states (similarly to normal optical measurements) but also about the electron spin polarization of states

participating in the magneto-optical transition.[16,17]

The temperature dependence for different MO effects measured at a definite wavelength indicates the variation of the magnetic order in the samples. Temperature and magnetic field dependences of MO effects reveal the phase transition temperatures and peculiarities of the originated magnetically ordered states. The MO response is sensitive not only to the long-range magnetic order but even to the short-range magnetic order. Thus, the formation of ferromagnetic clusters would manifest itself in the MO properties.

The phenomenological description of MO effects is based on consideration of the influence of a magnetic field on the dielectric permittivity tensor ε_{ij} of the medium.[17] If the tensor is symmetric ($\varepsilon_{ij}=\varepsilon_{ji}$) in zero magnetic field $H=0$, it becomes nonsymmetric $[\varepsilon_{ij}(H)=\varepsilon_{ji}(-H)]$ in a nonzero magnetic field. In the linear approximation, the dielectric permittivity tensor of the gyroelectric medium is

$$\tilde{\varepsilon}=\begin{Bmatrix} \varepsilon_0 & i\varepsilon_{xy} & 0 \\ -i\varepsilon_{xy} & \varepsilon_0 & 0 \\ 0 & 0 & \varepsilon_0 \end{Bmatrix}, \quad (1)$$

where the diagonal elements $\varepsilon_0=\varepsilon_0'-i\varepsilon_0''$ describe normal optical properties (which do not depend on magnetization) and off-diagonal elements $\varepsilon_{xy}=\varepsilon_{xy}'-i\varepsilon_{xy}''$, proportional to magnetization, are related to MO properties. All MO effects, which are linear in magnetization, can be expressed in terms of off-diagonal elements of the dielectric permittivity tensor.

For the TKE, variation of the reflected light intensity for *p*-polarized waves due to the magnetization of a ferromagnetic sample can be written as[17]

$$\delta_p=2\sin(2\varphi)\frac{A_1}{A_1^2+B_1^2}\varepsilon_{xy}'+2\sin(2\varphi)\frac{B_1}{A_1^2+B_1^2}\varepsilon_{xy}'', \quad (2)$$

where $A_1=\varepsilon_0''[2\varepsilon_0'\cos^2(\varphi)-1]$, $B_1=[\varepsilon_0''^2-\varepsilon_0'^2]\cos^2(\varphi)+\varepsilon_0'-\sin^2(\varphi)$, and φ is incidence angle of light.

The results presented in this article can be taken as supporting the transition of the Co^{3+} spins from the LS to the IS state with increasing temperature. Beside this, the results agree with the presence of the orbital ordering of the Co^{3+} ions in the IS state. For consideration of changes in the properties of the films with Sr doping the phase-separation effect is taken into account.

II. SAMPLES AND EXPERIMENTAL TECHNIQUES

The films (about 200 nm thick) were grown by pulsed-laser deposition onto a (001)-oriented $LaAlO_3$ substrate with a 1.06-μm Nd-YAG laser (pulse length 10 ns, pulse energy 0.33 J, pulse frequency 12 Hz). The ceramic targets with nominal compositions $La_{1-x}Sr_xCoO_3$ ($x=0.15,0.25,0.35$) were prepared by the solid-state reaction method. We were aware that available methods of chemical control can determine the actual compositions in targets and films with an accuracy not better than ± 2 at.%. Besides, the composition of pulsed-laser deposited films can differ slightly from that of the target. For all these reasons, the nominal compositions were chosen in such way that one of them ($x=0.15$) is sure below the percolation threshold ($x_c=0.20-0.25$),[9–11] at which the infinite FM cluster is formed below the Curie temperature in this system, the second ($x=0.25$) should be near the percolation threshold, and the third ($x=0.35$) is sure above this threshold. The results outlined in the following sections show that we have achieved this aim to a great extent.

At the ablation of target material, the substrate was shielded to avoid its direct exposure to the plasma plume. In this case deposition occurs from the flux that is reflected from a side screen. This has ensured a high surface smoothness, which is essential for obtaining reliable results at an optical study. The deposition was performed in oxygen atmosphere at a pressure of 8 Pa and substrate temperature of $880\pm 50°$ C. The deposited films were cooled to room temperature in oxygen at 10^5 Pa (1 atm). These preparation conditions make possible coherent epitaxy. Investigations of other cobaltite films, prepared in the same pulsed-laser deposition chamber and in the same conditions, provide reason enough to suggest that the films studied are polycrystalline, even if rather highly oriented.

The optical absorption spectra of the films were measured at 80–295 K with a prism infrared spectrometer (in the range 0.1–1.4 eV) and a grating spectrometer (in the range 1.0–4.0 eV). The measurements of the TKE were made using an automatic MO spectrometer.[18] A dynamic method to record the TKE was used. The relative change in the intensity of the reflected light, $\delta=[I(H)-I(0)]/I(0)$, where $I(H)$ and $I(0)$ are the intensities of the reflected light in the presence and absence of a magnetic field, respectively, was directly measured in the experiment. The magnitude of the alternating magnetic field in the gap of an electromagnet was up to 3.5 kOe. The relative precision of the apparatus is 10^{-5}. MO spectra were recorded in the photon energy range 1.3–3.8 eV at a fixed light incidence angle $\varphi=67°$. For MO measurements, a continuous-flow helium cryostat is used, which makes possible investigations in the temperature range 10–300 K.

The resistivity of the films was measured as a function of temperature and magnetic field (up to 20 kOe) using the standard four-point probe technique. The field was applied parallel or perpendicular to the film plane. In both cases it was perpendicular to the transport current.

III. EXPERIMENTAL RESULTS

A. Kerr effect

The temperature dependences of the TKE measured on $La_{1-x}Sr_xCoO_3$ films (in magnetic field $H=3.5$ kOe and at photon energy $E=2.8$ eV) are shown in Fig. 1. The $\delta(T)$ curves reveal characteristic features at the transition to the magnetically ordered state. The position of the abrupt decrease in the TKE on the temperature scale (when going from lower to high temperature) corresponds to the Curie temperature T_c. As follows from given curves, Curie temperatures for films with $x=0.35$ and $x=0.25$ coincide and are equal to 230 K. Below 230 K the films with $x\geqslant 0.25$ exhibit a considerable magneto-optical effect with a peak at

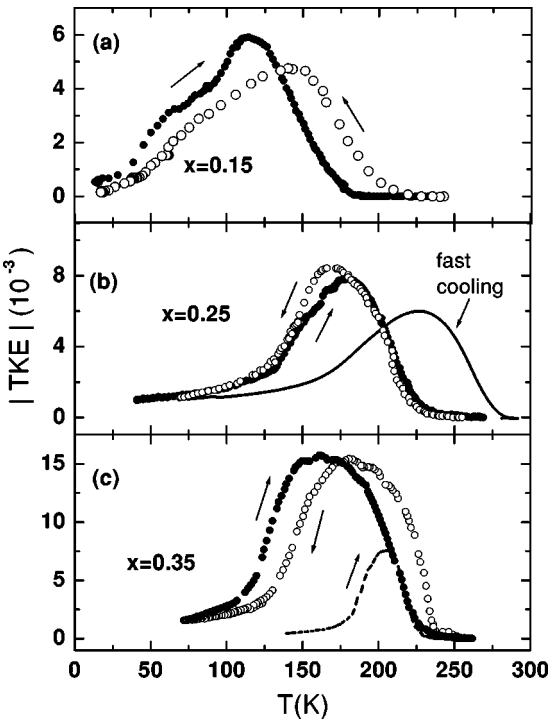

FIG. 1. Temperature dependences of the TKE of $La_{1-x}Sr_xCoO_3$ films with $x=0.15$ (a), $x=0.25$ (b), and $x=0.35$ (c). Heating and cooling regimes are indicated by arrows. All curves were recorded in magnetic field $H=3.5$ kOe at photon energy $E=2.8$ eV, except the dashed-line curve for $x=0.35$, which was recorded on heating in field $H=0.9$ kOe. The solid line in the picture for $x=0.25$ (b) corresponds to fast cooling. Rates of heating and cooling were usually in the range 1–3 K/min; the ''fast cooling'' was done with a rate about 20 K/min.

$T\approx180$ K. As the temperature decreases further, the TKE drops sharply: its value becomes more than 3 times smaller in the range 110–160 K for $x=0.35$ or in the range 130–175 K for $x=0.25$. For the film with $x=0.15$, the TKE has a peak at $T=118$ K and another anomaly at $T\approx60$ K. Note that in the low-temperature region ($T<118$ K), the TKE for $x=0.15$ is larger than for films with higher Sr concentrations. The $\delta(T)$ shape is dependent considerably on measurement conditions. As seen in Fig. 1, the TKE curves for $x=0.15$ and $x=0.35$ measured on cooling and heating in a high field ($H=3.5$ kOe) are shifted relative to each other. Hysteresis phenomena were much smaller for the film with $x=0.25$ and were observed only near the maximum.

The position of the maximum in the TKE temperature curve is dependent on the applied magnetic field and shifted to the high-temperature region when the field decreased. On heating the film with $x=0.35$ in the field $H=0.9$ kOe, the $\delta(T)$ curve shifts drastically (over 70 K) towards higher temperatures [Fig. 1(c)] when compared with the $\delta(T)$ curve taken in the higher field $H=3.5$ kOe. Both curves nearly coincide at $T>200$ K. On a fast cooling (with a rate about 20 K/min) of the film with $x=0.25$, the $\delta(T)$ curve shifts to the high-temperature region enormously and the maximum magnitude of the TKE decreases greatly [Fig. 1(b)]. At $T<110$ K, the TKE for films with $x\geqslant0.25$ decreases linearly with temperature (Fig. 1).

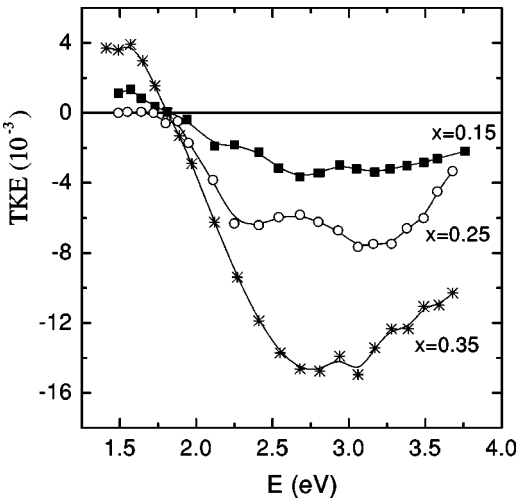

FIG. 2. Spectral dependences of the TKE of the $La_{1-x}Sr_xCoO_3$ films at temperatures of maximum in the temperature dependence of the TKE.

The spectral dependences of the TKE measured at temperatures of the maximum in their temperature curves are shown in Fig. 2. It is seen that the spectra are similar for all Sr concentrations studied. The Kerr effect has a positive maximum at $E\approx1.5$ eV and a broad negative maximum in the range of $E\approx2.7$ eV. The amplitudes of the peaks increase with growing Sr concentration. Above 2.0 eV the spectra exhibit a fine structure which is most distinct for the film with $x=0.15$ (peculiar features at 2.1, 2.6, and 3.1 eV stand out against the background of the broad maximum).

The field dependences of the TKE, $\delta(H)$, for the low-temperature range are linear for all films studied (Fig. 3). They are, however, quite different near the temperatures corresponding to a maximum in the $\delta(T)$ dependences. For the film with $x=0.15$ the $\delta(H)$ is linear up to 3.5 kOe, whereas for films with $x=0.25$ and $x=0.35$ it looks like a field-magnetization curve for FM compounds.

B. Resistivity and magnetoresistance

The temperature dependences of resistivity, $\rho(T)$, for the films studied are presented in Fig. 4 in semilogarithmic coordinates. Since the resistivity of the film with $x=0.35$ shows only a small visible temperature variation in this scale, it is presented more clearly in Fig. 5 in linear coordinates. The dependences $\rho(T)$ for films with $x=0.15$ and $x=0.25$ have nonmetallic character ($d\rho/dT<0$) (Fig. 4). They are found to be rather unusual: $\rho(T)$ follows closely the dependence $\rho(T)=\rho(0)\exp(-aT)$ for $x=0.15$ and is practically linear in temperature for $x=0.25$. The dependence $\rho(T)$ for $x=0.35$ has a maximum at $T\approx250$ K and a shallow minimum at $T\approx40$ K (Fig. 5). The minimum is most probably connected with a polycrystalline structure of the film.[19] The behavior of $\rho(T)$ is metallic between these extremum points.

The temperature dependences of the magnetoresistance (MR), $\Delta R(H)/R(0)=[R(H)-R(0)]/R(0)$, measured in the magnetic field $H=20$ kOe are shown in Fig. 6. It is seen

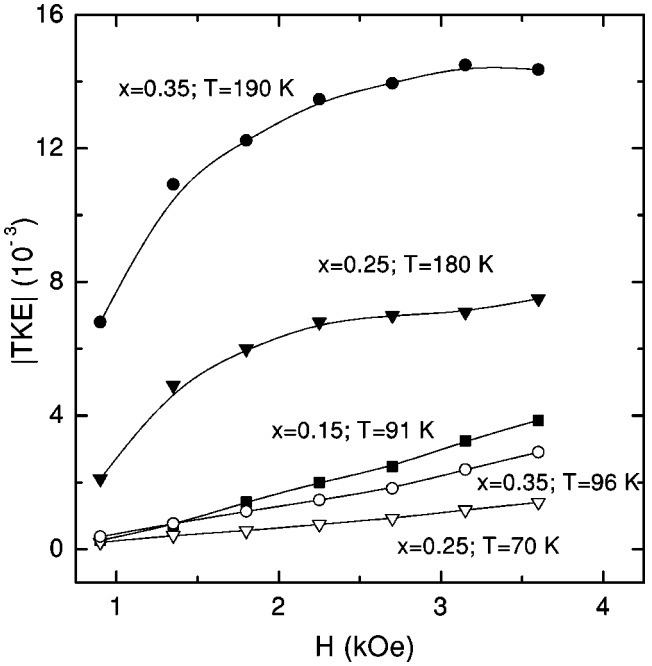

FIG. 3. Magnetic-field dependences of the TKE of the $La_{1-x}Sr_xCoO_3$ films studied at temperatures corresponding to the maximal TKE effect (190 K for $x=0.35$ and 180 K for $x=0.25$) and at much lower temperatures.

that for this field the MR is negative for all films studied. The dependence taken on the sample with $x=0.35$ is quite typical of optimally doped FM cobaltites and manganites [Fig. 6(a)]: there is a quite pronounced peak (in the MR modulus) near the Curie temperature $T_c \approx 230$ K; it goes down for temperatures deviating to either side from T_c. This type of MR behavior is characteristics of the so-called intrinsic mechanism of MR, which depends on the magnetic order (an external field enhances the magnetic order, which, in its turn, leads to a decrease in the resistivity and, therefore, to negative MR).

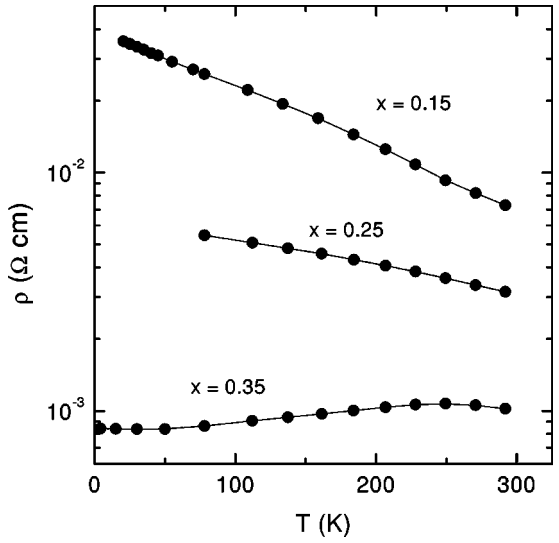

FIG. 4. Temperature dependences of the resistivity of the films $La_{1-x}Sr_xCoO_3$ (in semilogarithmic coordinates).

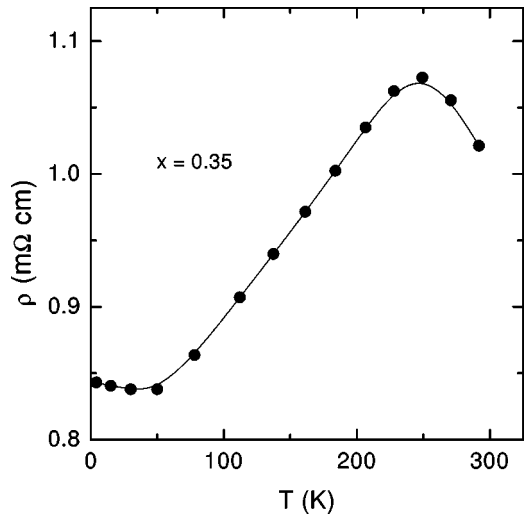

FIG. 5. Temperature dependence of the resistivity of film $La_{0.65}Sr_{0.35}CoO_3$.

This mechanism works in the FM state only. For this reason the MR decreases to zero for temperatures above T_c. Far below T_c, the MR of this type goes to zero as well since an applied magnetic field cannot strengthen the magnetic order

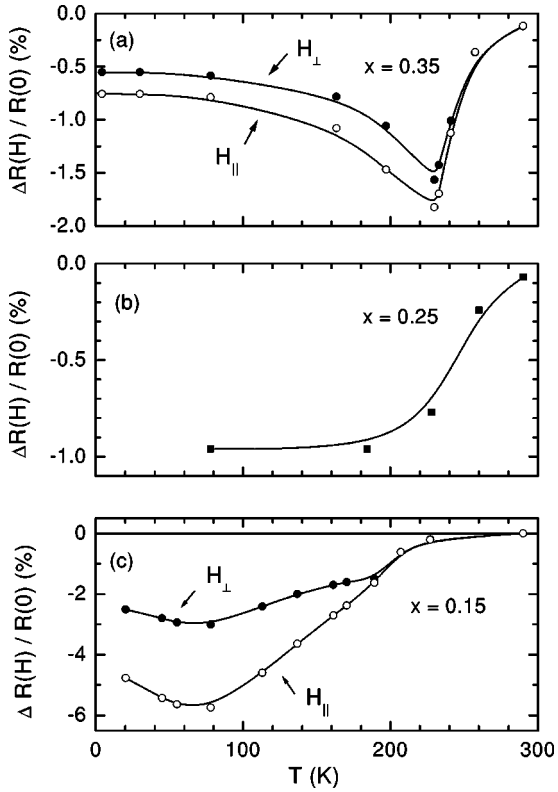

FIG. 6. Temperature dependences of magnetoresistance $[R(H)-R(0)]/R(0)=\Delta R(H)/R(0)$ at $H=20$ kOe of the $La_{1-x}Sr_xCoO_3$ films. The fields $H_\parallel$ and $H_\perp$ were applied parallel and perpendicular to the film plane, respectively. In both cases the fields were perpendicular to the transport current. The MR of the film with $x=0.25$ (b) has not shown a noticeable sensitivity to the angle between the field and film plane.

appreciably in the low-temperature range ($T \ll T_c$) where the magnetization is close to saturation.

In a magnetically inhomogeneous sample, consisting of weakly connected FM regions in a dielectric or nonmagnetic matrix, the so-called extrinsic mechanisms of MR can give an additional contribution to the total MR. These mechanisms are determined by the charge transfer between the poorly connected or isolated FM regions. This type of magnetic inhomogeneity in FM oxides can be connected with grain boundaries in polycrystalline samples or with the phase-separation effects. A contribution of the extrinsic MR increases with temperature decreasing and is maximum at zero temperature. A concurrence of the intrinsic and extrinsic MR's can result in a nonmonotonic temperature dependence of the total measured MR in cobaltite films.[19,20] Discussions of the possible mechanisms for the extrinsic type of MR in inhomogeneous polycrystalline samples can be found in Ref. 21. It is clear that these mechanisms are applicable (at least generally) also in the case of phase separation when this results in a system of hole-rich FM clusters embedded in a hole-poor dielectric matrix. In this way, the temperature behavior of MR in FM oxides can reflect their magnetic homogeneity. Taking it all into account, it can be said from Fig. 6(a) that film with $x=0.35$ is the most homogeneous from the films studied although even it has appreciable MR at the low-temperature range that indicates the presence of some magnetic inhomogeneity induced by one or both of the above-mentioned reasons. The MR of the film with $x=0.25$ increases continuously with decreasing temperature [Fig. 6(b)], which corresponds to the behavior of a highly inhomogenenous system. The same is true in relation to the films with $x=0.15$ where additionally a nonmonotonic temperature behavior of MR can be seen. It should be noted that the largest MR is observed in the least doped sample ($x=0.15$) [Fig. 6(c)]. For films with $x=0.15$ and 0.25, the temperature interval where MR increases with lowering temperature is fairly close to the temperature range of increasing TKE.

The MR of films with $x=0.35$ and $x=0.15$ is anisotropic (Fig. 6). The absolute values of negative MR are much higher in fields parallel to the film plane than in perpendicular ones. The anisotropic MR is not surprising for pulsed-laser deposited films of FM perovskite oxides. For cobaltites, this effect was seen earlier in $La_{0.5}Sr_{0.5}CoO_3$ film.[19] Since the conductivity in mixed-valence cobaltites increases with an enhancement of the FM order, this behavior just reflects the point that the magnetization increases more easily in a magnetic field parallel to the film plane. It is connected mainly with the shape anisotropy of the magnetization. The strain-induced anisotropy due to the film-substrate lattice interaction can have an influence as well. The influence of this type of MR anisotropy has been found in $La_{0.5}Sr_{0.5}CoO_3$ film.[20] All these types of the MR anisotropy are associated with the FM state and, for this reason, disappear above T_c. In the films studied, MR anisotropy is found only below $T \approx 200$ K for $x=0.15$ and below $T \approx 250$ K for $x=0.35$. The highest MR anisotropy is observed in the film with $x=0.15$ [(Fig. 6(c)]. No appreciable MR anisotropy is found in the film with $x=0.25$.

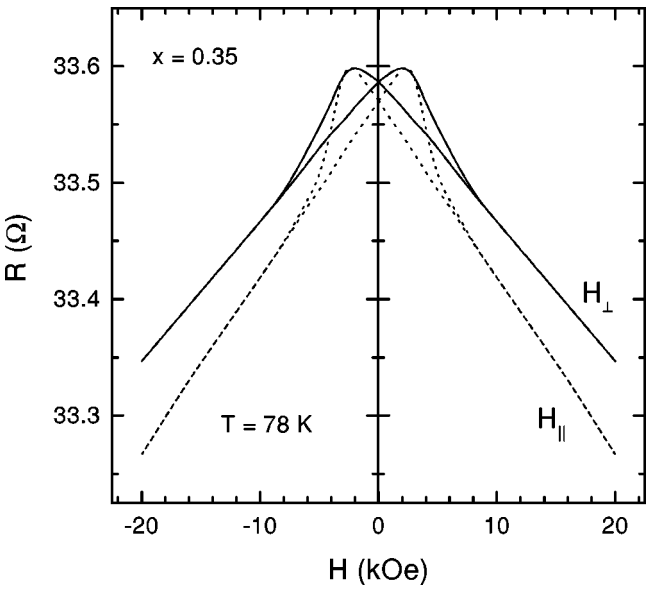

FIG. 7. Magnetoresistive hysteresis for $La_{1-x}Sr_xCoO_3$ film with $x=0.35$ at $T=78$ K. Applied fields were parallel ($H_\parallel$) and perpendicular ($H_\perp$) to the film plane. In both cases the fields were perpendicular to the transport current.

Generally, the MR curves of the films studied have been hysteretic with specific structures in low fields (see Fig. 7 for $x=0.35$ at $T=78$ K). It is well established that the behavior of the MR curves for FM oxides correlates with that of magnetization curves.[21] In particular, the field $H=H_p$, where the resistance reaches its maximum (Fig. 7), corresponds to the coercive force H_c. It is found that the field H_p is maximal at the lowest temperature in this study ($T \approx 4.2$ K) but drops to zero above $T \leqslant 77$ K for $x=0.15$ and above $T \approx 90$ K for $x=0.35$. Above certain field values, hysteresis no longer occurs, which implies that magnetization reversal processes start in these fields. Such fields are much lower for the parallel orientation (Fig. 7). We will discuss the hysteresis phenomena more elaborately below.

C. Optical absorption

The optical density spectra $D=\ln(I_0/I) \equiv \ln(1/t)$ (I_0 is the incident-light intensity, I is the intensity of light transmitted through the films, and t is the transmittance) in the visible and infrared (IR) ranges are shown in Figs. 8 and 9, respectively. The optical density spectrum (corresponding to the absorption spectrum where the reflection and film thickness was not taken into account) for the film with $x=0.15$ has a wide band at $E \approx 3.0$ eV and quite narrow bands at about 1.15, 1.9, and 2.4 eV in the fundamental absorption region (Fig. 8). When the Sr concentration is increased, the low-energy band (1.15 ± 0.03) eV shifts slightly towards higher energies. For $x=0.35$ it is centered at 1.3 eV. The 1.9-eV band broadens and shifts towards lower energies.

For the film with $x=0.15$, absorption in the IR range goes up for energy increasing above 0.9 eV (Fig. 9), which indicates the onset of fundamental absorption. At $E<0.9$ eV the light interaction with charge carriers contributes to the ab-

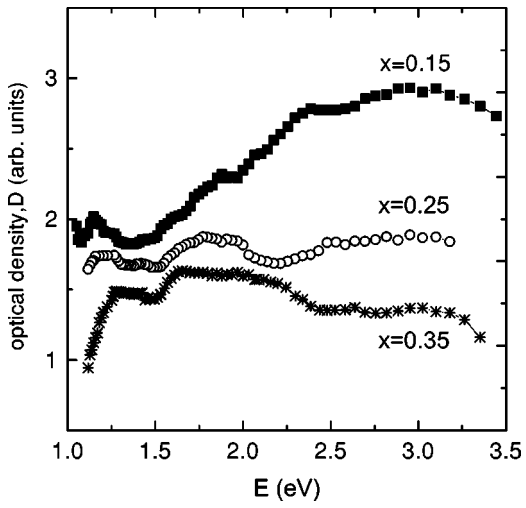

FIG. 8. Optical density spectra $D=\ln(I_0/I)$ (I_0 is the incident-light intensity, and I is the intensity of light transmitted through the film) for $La_{1-x}Sr_xCoO_3$ films studied in the visible light range at $T=295$ K. The curves are spaced apart for facilitation of visual perception.

sorption of the films with $x=0.25$ and $x=0.35$. As follows from the reflection spectra for $LaCoO_3$,[22] phonon absorption begins below 0.08 eV.

The absorption in the film with $x=0.15$ is considerably lower at 80 K than at 295 K in the IR range (Fig. 9). For the film with $x=0.25$ the absorption in the region $E<0.9$ eV is

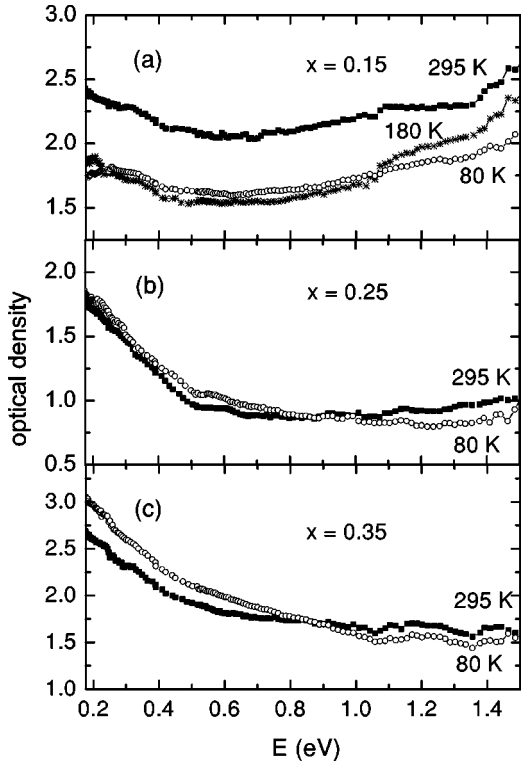

FIG. 9. Optical density spectra $D=\ln(I_0/I)$ (I_0 is the incident-light intensity, and I is the intensity of light transmitted through the film) for $La_{1-x}Sr_xCoO_3$ films studied in the IR range at different temperatures.

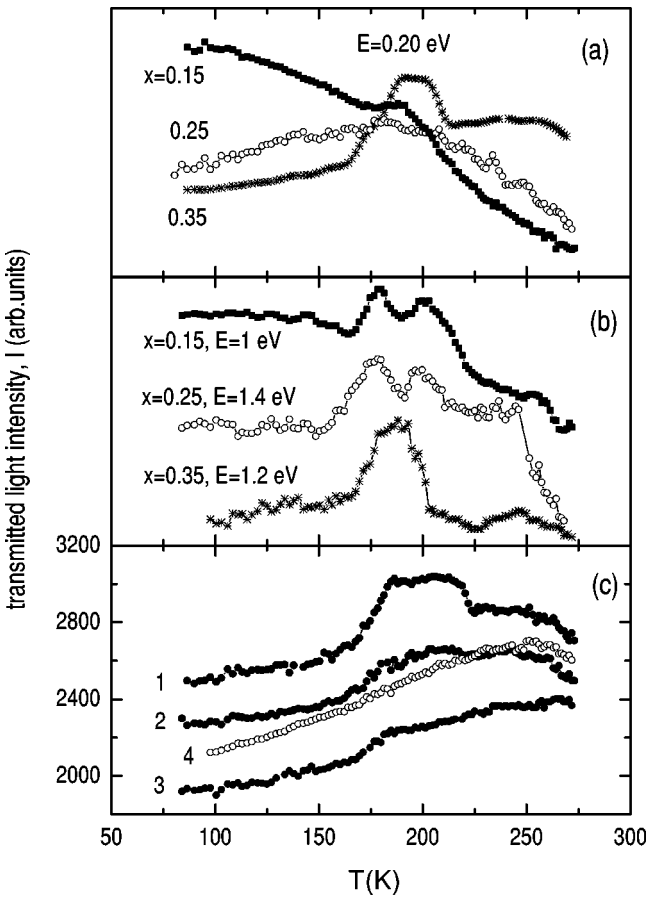

FIG. 10. Temperature dependences of the intensity of light transmitted through the $La_{1-x}Sr_xCoO_3$ films at $E=0.20$ eV (a) in the energy range 1.0–1.4 eV (b) and for different measurement conditions at $E=0.20$ eV for film with $x=0.35$ (c). The numerals in panel (c) of the figure indicate the following: (1) ZFC, $H=0$; (2) FC, $H=0$; (3) ZFC, $H=8$ kOe; and (4) fast cooling after a heating up to $T=320$ K, $H=0$ (heating with the rate about 1–1.5 K/min; the following ''fast cooling'' from 320 K to $T\approx80$ K have taken about 10 min). The curves in panels (a) and (b) are spaced apart for facilitation of visual perception.

slightly higher at 80 K than at 295 K. For the film with $x=0.35$ the absorption at $E<0.9$ eV is considerably higher at 80 K than at room temperature, which implies that the contribution of charge carriers to the spectrum is larger for $x=0.35$ than for $x=0.25$.

As shown for manganites,[14,15,23] in the energy range of light interaction with charge carriers, the behavior of $t(T)$ [or transmitted light intensity $I(T)$] follows the temperature behavior of resistivity in the case that the metallic FM region percolates through the whole material. For the manganites, which for some reasons consist of separated metallic regions embedded in a semiconducting matrix, the $I(T)$ dependence reflects the temperature behavior of the resistivity in these isolated metallic regions (or clusters) and this behavior can be quite different from the direct-current $\rho(T)$ dependences. The $I(T)$ behavior in Sr-doped cobaltite films at $E=0.20$ eV is shown in Fig. 10(a). On cooling the transmitted light intensity (transmittance) of the film with $x=0.15$ increases; i.e., the transmittance behavior is semiconductive at

80–300 K. In the film with $x=0.25$ the transmittance exhibits metallic temperature behavior at $T<180$ K, although no behavior of this type can be seen in the $\rho(T)$ dependence (Fig. 4). In the film with $x=0.35$ transmittance drops significantly below $T\simeq 250$ K (metallic behavior), which is in agreement with the $\rho(T)$ behavior for this film (Fig. 5).

The $I(T)$ dependences of cobaltite films studied have an extra anomaly (most pronounced for $x=0.35$) in the same temperature range 160–220 K (Fig. 10). This type of anomaly was never seen in manganites. The anomaly is observed not only at the photon energy range where light interaction with charge carriers occurs [Fig. 10(a)], but at the range of the fundamental absorption edge at $E=1.0$–1.4 eV [Fig. 10(b)] as well, where only small ($x=0.25$, $x=0.35$) or no ($x=0.15$) contribution of charge carrier to absorption is expected. The anomaly is more complicated at $E=1.0$–1.4 eV [Fig. 10(b)] than at $E=0.20$ eV [Fig. 10(a)]. This may be connected with the intricate character of the spectrum near the fundamental absorption edge, where the closely spaced and spectrally unresolved absorption bands overlap. Note that in our experiments the spectral bandpass of slits in the two spectrometers used is different in the region of overlapping working ranges. The spectra in Fig. 8 measured with a smaller spectral bandpass are therefore resolved better than the spectra in Fig. 9.

The magnetotransmittance effect (analogous to magnetoresistance) detected in manganite films[24] is not found in cobaltite films studied up to $H=10$ kOe apparently because cobaltites have much lower magnetoresistance. The influence of magnetic fields on transmittance of the films shows up itself, however, in rather different behavior of the $I(T)$ curves taken at $E=0.20$ eV on cooling in zero and finite ($H=8$ kOe) fields. The strong effect of the sample thermomagnetic prehistory is illustrated in Fig. 10(c). Curves 1–4 describe the $I(T)$ dependences under successive changes in measurement conditions. The $I(T)$ anomaly weakened on field cooling (FC) and measurement in $H=0$ (curve 2) or on zero-field cooling (ZFC) and measurement in $H>0$ (curve 3). The anomaly is suppressed completely when the film is heated above room temperature and then cooled quickly (curve 4). Additional explanatory comments to the measurement conditions can be found in caption to Fig. 10.

IV. DISCUSSION

A. Absorption spectra and Kerr effect

There are only scanty optical studies on $La_{1-x}Sr_xCoO_3$.[6,22,25–27] Found among them are optical conductivity spectra obtained by a Kramers-Kronig analysis of the reflectivity spectra of polycrystals and single crystals.[26] The polar Kerr effect for $La_{1-x}Sr_xCoO_3$ single crystals at room temperature was studied in Ref. 27. The optical density spectra $D(E)$ of the films studied have more features in the visible range (Fig. 8) than the light conductivity spectra $\sigma(E)$ of $La_{1-x}Sr_xCoO_3$ single crystals with similar composition.[26] The $\sigma(E)$ spectra of single crystals have three bands at energies about 1, 3, and 6 eV, respectively.[26] They are attributed[28] to excitations into the e_g band from the t_{2g} band and a broad O($2p$) band split by hybridization effects into bonding and antibonding parts. The spectra of the cobaltite films studied have four bands in energy range 1.0–3.5 eV (Fig. 8). This can be presumably attributed to the superposition of geometric resonances (surface plasmons) induced by structural inhomogeneities on charge transfer transitions (as shown for manganites in Ref. 29). Inhomogeneous structures may appear due to the phase separation, polycrystallinity of the films, and strains at the film-substrate boundary. The evolution of absorption spectra with doping for the films studied is similar to that of single crystals[26]: as the Sr concentration increases, the spectral weight transfers from the visible range to the IR region, where light interaction with free charge carriers occurs.

The TKE magnitude is comparable in cobaltites (Fig. 2) and manganites.[27] The high value of the Kerr effect may be connected with the strong spin-orbit interaction expected for Co^{3+} (IS) ions. As for $La_{1-x}Sr_xCoO_3$ single crystal,[27] the TKE in the films studied was maximum in the broadband near 3.0 eV. In Ref. 27 this behavior was attributed to the d-d transition $t_{2g}\rightarrow e_g^*$ allowed for the majority-spin (or spin-up) states because of the hybridization with O($2p$) orbitals. The large MO effect found in the films studied may also be related to this transition, which must take place only for Co^{3+} ions in the IS or HS state, but not in the LS state. Qualitatively, the TKE behavior can also be explained on the basis of a band calculation for $LaCoO_3$ with Co^{3+} (IS) ions.[3] According to the electron-energy scheme for Co ions in the IS state,[3] the magneto-optical effect should first appear in the spin-up subband and reach its maximum at $E\approx 2.0$ eV. Then, at $E>3.5$ eV the transitions in the spin-down subband can be expected. The competition of these transitions can also account for the change in sign and spectral behavior of the effect.

B. Temperature dependences of the transmittance, Kerr effect, resistivity, and magnetoresistance

It is found for lanthanum manganites of varying compositions[14,15] that the temperature at which the FM contribution appears (estimated from the temperature dependences of the TKE) agrees well with the temperature of the insulator-metal transition in the hole-rich separated regions or clusters (found from IR absorption data). A direct correlation of this type is not seen in the cobaltite films studied [compare Figs. 1 and 10(a)]. We will try in the following to clear up a possible reason for this discrepancy. In doing so we can assume that the holes appearing with Sr doping of cobaltites cause phase separation into hole-poor matrix and hole-rich regions (e.g., see Refs. 9,10, and 13).

1. $La_{0.85}Sr_{0.15}CoO_3$ film

Our magneto-optical, optical, MR, and MR anisotropy results for the film with $x=0.15$ support the outlined general picture for magnetic processes in cobaltites with low doping level below the percolating threshold ($x_c=0.20$–0.25).[9–11] The monotonic (except for the range 160–220 K) temperature dependence of intensity of the transmitted light at $E=0.20$ eV in the film with $x=0.15$ [Fig. 10(a)] suggests that

the clusters with Co^{4+} ions are rather small in size and their volume fraction is much less than that of the semiconducting matrix. For this reason, apparently, the transition of these isolated clusters to a more conductive FM state with decreasing temperature does not show itself either in $I(T)$ [Fig. 10(a)] or in $\rho(T)$ (Fig. 4) dependences. The TKE value characterizing the FM contribution is, however, quite high—only 3 times less than that for $x=0.35$. The TKE has a maximum at 118 K. After cooling in zero field, another feature (a shoulder) appears at $T\simeq 60$ K [Fig. 1(a)]. A maximum at nearly the same temperature $T_g=60-70$ K was found earlier in the temperature dependences of the ac and dc susceptibility for bulk $La_{0.85}Sr_{0.15}CoO_3$ (Refs. 9,10,12, and 13) and attributed to spin-glass freezing. Magnetization temperature curves for $La_{0.85}Sr_{0.15}CoO_3$ show a cusp at the same freezing temperature T_g.[11,30] It can be thought that the above-mentioned feature in the TKE temperature curve near the temperature $T\approx 60$ K [Fig. 1(a)] is determined by the same effect.

It should be noted that the highest MR and its anisotropy for this film are observed in the range 60–80 K [Fig. 6(c)]. The ratio of MR's measured in fields parallel and perpendicular to the film plane is close to 2. At $T=4.2$ K and 20.4 K the values of field H_p are found to be rather high ($H_{p\parallel}=7.0$ kOe and $H_{p\perp}=4.5$ kOe for field orientation parallel and perpendicular to the film plane, respectively). At $T=78$ K and above MR hysteresis is practically unobservable. Taking into account that the field H_p is equal to the coercive force H_c (see Sec. III B above) this behavior is quite consistent with the assumed cluster-glass state at this doping level. A cluster glass is actually a system of small FM (single domain) particles. An isolated particle should have enough thermal energy to surmount the energy barrier $\Delta E=KV$ (K is the anisotropy constant, and V is the particle volume) to reverse its magnetization in a magnetic field.[31,32] For a system of such particles there is the so-called blocking temperature T_B, below which the particle moment is blocked. The mean blocking temperature $\langle T_B\rangle \propto K_m V_m$ is determined by mean values (K_m and V_m) of the anisotropy constant and particle volume.[31] The above-mentioned temperature T_g is directly related to $\langle T_B\rangle$ by relation $T_g=\beta\langle T_B\rangle$,[31] where β is a numerical factor of the order of unity depending on the form of the particle size distribution. The higher the temperature, the smaller H_c. According to Ref. 32, $H_c\propto(1-T/T_B)^{1/2}$, so that at $T>\langle T_B\rangle$ the system becomes superparamagnetic. It is therefore most probable that the linear magnetic-field dependence of TKE in this film at $T=91$ K (near the Kerr effect maximum) (Fig. 3) is determined by the superparamagnetic behavior of the clusters. The high H_p field for the film with $x=0.15$ agrees with the H_c data obtained on a bulk polycrystal of the same composition.[30]

The FM interaction in clusters is mainly attributable to the Co^{3+}(IS)-O-Co^{4+}(LS) superexchange or the double exchange of localized t_{2g} electrons via itinerant e_g electrons.[9] As another source of the FM state, the magnetic polarons formed near the Co^{4+} ions can be mentioned.[22] The hole-rich regions stabilize the IS state of Co^{3+} ions at the interface to the hole-poor regions. The clusters are thought to be coupled antiferromagnetically (AFM) through the superexchange interaction between the Co^{3+} (IS) ions.[9] Since the clusters are distributed randomly, the intercluster exchange is frustrated and the cluster moments have noncollinear orientation. This leads to a large anisotropy below the temperature T_g. The influence of all these factors on magnetic properties can show itself as a typical spin-glass-like behavior.

Among the films studied, this film has the highest MR [Fig. 6(c)]. It is difficult to imagine that strengthening of the magnetic order in small isolated clusters embedded in a semiconducting matrix can cause this rather strong effect.[19] It should be suggested, therefore, that an applied magnetic field enhances the intercluster tunneling and/or increases the conductivity of intercluster semiconducting regions. It is quite probable that the magnetic field affects somehow the interface regions between the hole-rich clusters and hole-poor matrix (which are enriched with Co^{3+} ions in IS state[9]). It was argued in Ref. 10 that the volume of the superparamagnetic clusters should increase in a magnetic field, which can cause a considerable MR effect. These suggestions need, however, an elaboration and verification in a further study.

2. $La_{0.75}Sr_{0.25}CoO_3$ film

When the Sr concentration is raised to $x=0.25$, the content of holes in clusters increases. The volume of the FM clusters increases too, and the exchange in them is enhanced by charge carriers (double exchange). A decrease in transmittance with temperature decreasing on cooling below the temperature of the metal-insulator transition, $T_{MI}\simeq 180$ K [Fig. 10(a)], together with no signs of the transition to metallic state at this temperature in $\rho(T)$ dependence (Fig. 4) indicates that in the film with $x=0.25$ the transition to a FM metallic state near 180 K occurs only in the isolated hole-rich clusters (embedded in a semiconducting matrix) rather than in the whole volume of the film. For this reason there are no continuous metallic conducting paths penetrating the whole film and, therefore, the transition of the clusters to the FM state has no visible effect on the recorded $\rho(T)$ behavior (Fig. 4). But this transition is reflected in the MR temperature behavior which is shown in Fig. 6(b). It can be seen that the MR reaches its maximum below $T\simeq 200$ K which agrees well with the magneto-optical and optical data obtained [see Figs. 1(b) and 10(a)]. Generally, the temperature behavior of MR for this film corresponds to that of a highly inhomogeneous magnetic system, as was mentioned already in Sec. III B.

No significant MR anisotropy or MR hysteresis has been found in this film. It is caused, perhaps, by the proximity of the composition to the percolation threshold ($x_c=0.20-0.25$), near which cluster sizes and orientations are most chaotic. The TKE appears at $T\simeq 230$ K, i.e., above the temperature $T_{MI}\simeq 180$ K obtained from the transmittance data. The relation $T_{MI}<T_c$ is expected for this range of Sr doping.[10] The field dependence of the TKE (Fig. 3) exhibits a typical FM behavior at the temperature ($T\approx 180$ K) where the TKE is maximum, but is linear at $T=70$ K, which is typical of a superparamagnetic system, but can also be determined by a change in the relationship between the FM and

AFM contributions responsible for the magnetism of this film with lowering temperature.

3. $La_{0.65}Sr_{0.35}CoO_3$ film

For $x > x_c$, the volume fraction of hole-rich regions should be high enough to form an infinite percolating FM cluster below T_c.[9] The results for the film with $x = 0.35$ support well this view. Both $\rho(T)$ and $I(T)$ dependences [Figs. 5 and 10(a)] manifest that the metal-insulator transition starts at $T \approx 250$ K. The temperature behavior of the MR is typical of optimally doped cobaltites, with a sharp maximum at $T = 230$ K which corresponds to the Curie temperature for this film. At that, the metallic behavior of $I(T)$ is more pronounced than for $x = 0.25$, but a strong anomaly can be seen in the range 160–220 K. The maximum Kerr effect is found to be larger for $x = 0.35$ than that for $x = 0.25$, and the temperature range of maximal Kerr effect magnitude is wider [Fig. 1(c)]. At the same time the magnitude of the Kerr effect drops sharply below 160 K. The same as for $x = 0.25$, the field dependence of the TKE (Fig. 3) exhibits a typical FM behavior for the temperature range where $\delta(T)$ is maximum, but is linear at $T = 96$ K.

Although at $x = 0.35$ the infinite FM cluster, percolating through the whole sample, is formed, at the same time, however, a pervasive hole-poor matrix with some isolated clusters in it persists up to $x = 0.5$.[9] The large cluster interfaces and/or the interlayer between the FM grains contain Co^{3+} (IS) ions which change into the LS state with lowering temperature and no longer assist the charge transport and Kerr effect. As the number of Co^{3+} (IS) ions is reduced and the related FM interaction grows weaker, the carriers can gradually localize in the FM clusters themselves. This mechanism is maybe responsible for the rather high resistivity of the film with $x = 0.35$ below $T = 50$ K and for the hysteretic and anisotropic behavior of MR. The low-temperature resistance minimum is typical of polycrystalline samples with weak enough interconnections between FM grains. In this case the intergrain tunneling can become activated at low enough temperature, which leads to a nonmetallic behavior of $\rho(T)$.[19] It is clear that the magnetical inhomogeneity due to the phase separation can contribute to this effect in the same way as polycrystalline structure. The MR hysteresis is found to be absent above 90 K, but fields H_p are significant already at $T = 78$ K ($H_{p\parallel} = 2.5$ kOe and $H_{p\perp} = 2.0$ kOe). With temperature decreasing down to $T = 4.2$ K, the H_p values have increased up to $H_{p\parallel} = 4.5$ kOe and $H_{p\perp} = 5.3$ kOe. The strong decrease in the TKE and change in character of the field dependence of it for decreasing temperature, together with rather high MR anisotropy and the considerable growth of H_p in the low-temperature range, indicate that in spite of metallic behavior of the film conductivity, the FM state in it is not homogeneous and maybe close to a cluster-glass state.

C. Transmittance anomaly and orbital ordering of Co^{3+} (IS) ions

The features of the temperature and spectral behavior of optical and magneto-optical properties, considered above, can be determined by the transition of Co^{3+} ions from the LS state to either or both HS and IS states. In the transmittance spectra, however, a special anomaly is found, which can be attributed only to the LS-IS transition. This anomaly in the $I(T)$ dependence (kinked behavior of it) is observed for all films studied and appears practically in the same temperature range 160–220 K [Fig. 10(a)]. It can be seen quite clearly for films with $x = 0.15$ and $x = 0.35$ on the background of the general semiconductive or metallic run of their $I(T)$ curves. For the film with $x = 0.25$ the temperature range of the anomaly nearly coincides with the temperature T_{MI} and, therefore, the anomaly is not so distinct. An anomaly of this type is never mentioned for manganites. It is reasonable, therefore, to assume that its nature is determined by some specific feature of cobaltites. This is the transition of Co^{3+} ions from the LS state to a higher-spin state with increasing temperature. According to Ising-model molecular-field calculations, an energy gap $\Delta = 230$ K between the $S = 0$ and $S = 1$ spin states provides a good description of the temperature dependence of the magnetic susceptibility.[26] The spin transition proceeds gradually. No information can be found in the literature about the special temperature points of this transition, except for the Mössbauer effect in $LaCoO_3$.[33] The latter data permit the conclusion that the ratio between the Co^{3+} (HS) concentration and the total Co^{3+} content reaches its maximum at $T \simeq 200$ K. It follows, however, from neutron scattering data for $LaCoO_3$ (Ref. 10) that the 50:50 ratio of low-spin and higher-spin Co^{3+} ions is stable in a wide interval from 110 K to room temperature, which is supported by the results for magnetic susceptibility.[34]

According to electron structure calculations for $LaCoO_3$,[3] with rising temperature the LS ($S = 0$) state of Co ions transfers to the IS ($S = 1$) state rather than to the HS ($S = 2$) one. Energetically, the latter state appears to be higher than the IS state even above $T \simeq 600$ K. The Co^{3+} (IS) ion with the $(t_{2g}^5 e_g^1)$ configuration is a Jahn-Teller (JT) ion. In the case of equal spins, the orbitally ordered (nonmetallic) state is more preferable than the state without orbital order.[3] In this case the nonmetallic behavior of $LaCoO_3$ at $90\ \text{K} < T < 500$ K can be described properly assuming that Co^{3+} ions are in the orbital-ordered state. The gradual transition to the metallic behavior observed experimentally at $T > 550$ K is associated with destroying the orbital order.[3] The presence of JT Co^{3+} (IS) ions in cobaltites is supported by experimental results, such as anomalous splitting of phonon modes in $LaCoO_3$ (Ref. 6) and giant anisotropic magnetostriction in $La_{1-x}Sr_xCoO_3$ (Ref. 35). Measurement of magnetic circular dichroism spectra has revealed the presence of Co^{3+} (IS) ions with a finite orbital moment.[36]

It is possible that the $I(T)$ anomaly appears because the orbital-ordered Co^{3+} (IS) ions reach their maximum concentration at $T \simeq 180$ K. At $T > 180$ K the ions transfer gradually into the orbital-disordered state. The anomalous splitting of phonon modes in the spectrum of $LaCoO_3$ (Ref. 6) strengthens this hypothesis. The mode corresponding to the orbital-ordered state becomes saturated at $T \simeq 200$ K whereas the intensity of the mode ascribed to the orbital-disordered state increases sharply above $T \simeq 160$ K.

As the LS-IS transition occurs in some fraction of the Co ions, two features are expected in the optical spectra of mixed-valence cobaltites: (i) the appearance of new absorption lines corresponding to the optical transitions including energy states of Co (IS) ions and (ii) charge-carrier localization caused by JT lattice distortions near Co^{3+} (IS) ions, which may entail the formation of JT polarons. The intricate $I(T)$ dependence near the absorption edge (1.0–1.4 eV) [Fig. 10(b)] is determined, probably, by the appearance of additional absorption bands, which, however, are not resolved in this spectral range. These bands can have different temperature dependences, including the anomalous ones, and their superposition would result in tangled appearance of $I(T)$ dependence.

A possible reason for the $I(T)$ anomaly in the region of light interaction with the charge carriers at $E=0.20$ eV [Fig. 10(a)] can be charge localization at the maximum concentration of the orbital-ordered JT Co^{3+} (IS) ions. It is natural to assume that the orbital-ordered Co^{3+} (IS) ions reside in the hole-poor matrix (for $x=0.15$ and 0.25) or in the regions near the boundaries of hole-rich clusters (for $x=0.35$). The hole-rich clusters are expected to contain orbital-disordered Co^{3+} (IS) ions. The $I(T)$ anomaly can appear only when contributions of these two mechanisms—enhancement of the metallic behavior of charge carriers in the clusters and localization of charge carriers in the matrix—are comparable. It should be noted that this mechanism of charge-carrier localization is possible only for JT ions in a semiconducting matrix—that is, for Co (IS) ions. There is no such mechanism for LS-HS transitions of Co^{3+} ions. Cooling in a finite applied field or cooling at $H=0$ and subsequent measurement at $H>0$ suppresses the anomaly in $I(T)$, i.e., enhances the metallic contribution of the charge carriers [see Fig. 10(c) for $x=0.35$]. The anomaly is affected most significantly by a fast cooling of the film preheated to $T=320$ K [Fig. 10(c)]. At this temperature a significant fraction of Co^{3+} (IS) ions in the semiconducting matrix becomes orbital disordered. On fast cooling this ''disordered'' (and more metallic) state is frozen. After such thermal treatment the $I(T)$ anomaly vanishes completely both at $E=0.20$ eV (Fig. 10) and at $E=1.0$ eV (not shown). The metallic contribution becomes more pronounced as well. The appearance and change in number of orbital-ordered Co^{3+} (IS) ions in a dielectric matrix can be responsible for the unusual behavior of the TKE temperature dependence for films with $x\geqslant 0.25$ as well.

At $T=80$ K, the Kerr effect is equally small in films with $x=0.25$ and $x=0.35$, and it is smaller than in the film with $x=0.15$ (Fig. 1). This is because only a small fraction of Co^{3+} (IS) ions are involved in the FM exchange at 70–90 K. In films with $x\geqslant 0.25$, Co^{3+} (IS) ions are fewer than in the film with $x=0.15$ if we assume that the highest Co^{3+} (IS) concentration is 50% of all Co^{3+} ions both in nondoped $LaCoO_3$ and doped $La_{1-x}Sr_xCoO_3$. Besides, it is likely that in the matrix and in the boundary regions of metallic clusters the Co^{3+} (IS) ions are in the orbital-ordered state, so they interact antiferromagnetically. As a result, the number of the ions involved in the FM interaction is much less than 50% of the total Co^{3+} content corresponding to the nominal film composition. The linear behavior of the TKE as a function of magnetic field which is observed in all films below the TKE peak (Fig. 3) shows that the FM interaction (double exchange) weakens, and concurrence of the FM interaction (in clusters) and AFM interaction (in the matrix or boundary regions) comes into play.

An unusual fact is observed for the film with $x=0.35$: on heating in a weak field ($H=0.9$ kOe), the TKE dependence shifts significantly towards higher temperature when compared with that at $H=3.5$ kOe [Fig. 1(c)]. This finding implies that when the Kerr effect is measured in a magnetic field of 3.5 kOe, the Co^{3+} (LS)-Co^{3+} (IS) transition is driven not only by temperature but by the magnetic field as well. The spin transition should actually occur at higher temperatures, and the magnetic field stimulates its onset at lower temperatures. This conclusion was arrived at in Ref. 35, explaining the giant anisotropic magnetostriction of $La_{1-x}Sr_xCoO_3$ ($x=0.3$). The curves obtained for the film with $x=0.35$ are shifted after heating and cooling in a strong field [Fig. 1(c)] because heating stimulates an earlier onset of the LS-IS transition and cooling ''freezes'' the state which existed at high temperature. The temperature hysteresis of the TKE is small at $x=0.25$ presumably because the onset of FM and metal-insulator transition in clusters takes place within the interval $T=180$–200 K, where the content of orbital-ordered JT ions and, hence, the related AFM contribution are the highest. The state without orbital order has a larger magnetic moment,[3] which affords a strong TKE even above the temperature of the metal-insulator transition. The considerable TKE shift towards higher temperatures caused by fast cooling of the film with $x=0.25$ [Fig. 1(b)] agrees well with the effect produced by fast cooling on the $I(T)$ curves [Fig. 10(c)]. The fast cooling of the film which is partially in the orbital-disordered state (at $T\geqslant 300$ K) is favorable for ''freezing'' this state. As a result, the carrier localization weakens, the AFM component decreases, and the FM contribution increases.

The evolution of optical, magneto-optical, and transport properties of the films studied with the doping level correlates well with the concept of electron phase separation in cobaltites. At a low doping level ($x=0.15$), the Co^{3+} (LS)-Co^{3+} (IS) transition in the magnetic field begins at helium temperatures. The transition enhances the FM contribution in the clusters, which is mainly connected with the Co^{3+}- (IS) O-Co^{4+} (LS) superexchange. As a result, the Kerr effect grows up to $T=118$ K. On a further rise of temperature the number of Co^{3+} (IS) ions increases. The content of orbital-ordered ions in the matrix increases too and so does the related AFM contribution. In the temperature region where the content of the orbital-ordered Co^{3+} (IS) ions is the highest ($T\simeq 180$ K), the AFM contribution exceeds the FM one from the clusters and the Kerr effect turns to zero. The high coercive forces are indicative of the small sizes of the FM clusters in the nonmagnetic matrix. The magnetic state of the film with $x=0.15$ has doubtless features of the spin-glass state.

On a doping level ($x=0.25$) near the percolation threshold, the hole-rich FM clusters are quite numerous, but segregated. No infinite cluster is formed yet. In the clusters the

metal-insulator transition occurs near 180 K. This suggest that below 180 K the FM interaction is mainly connected with the charge carrier exchange (double exchange). Because of doping, the total content of Co^{3+} ions is smaller than at $x=0.15$ and the Kerr effect is also smaller at low temperatures. It is likely that the fraction of the orbital-ordered Co^{3+} (IS) ions grows with temperature only in the matrix and becomes the highest at $T\simeq 180$ K. Since the degree of orbital ordering decreases above this temperature, the TKE remains appreciably strong up to $T=230$ K because the state without orbital ordering has a large moment.

At the doping level ($x=0.35$) above the percolation threshold, the FM regions percolate magnetically as well as conductively through the whole film. For this reason the temperature of the metal-insulator transition is close to $T_c=230$ K. Although the number of Co^{3+} ions involved in the LS-IS transition decreased, the TKE maximum is much higher than at $x=0.25$ because the double exchange assisted by Co^{4+} ions enhances the FM contribution. The film is, however, magnetically inhomogeneous, which is evident from the TKE hysteresis under the heating-cooling condition. The considerable hysteresis and strong dependence of the TKE on the sample prehistory and thermal treatment may be connected with orbital ordering in the cluster interfaces, which are the sources of the AFM contribution. As in the $x=0.25$ case, the FM state of the film with $x=0.35$ below the temperature of the TKE maximum becomes much weaker due to the enhanced AFM interaction. This is evident from the sharp growth of H_c with decreasing temperature typical of the cluster glass state.

V. CONCLUSION

Optical, magneto-optical, and transport properties of polycrystalline $La_{1-x}Sr_xCoO_3$ ($x=0.15,0.25,0.35$) films have been studied. Unlike manganites, no direct correlation is found between the temperature of the metal-insulator transition in clusters and the temperature at which the FM contribution appears. It is found that the temperature dependences of the optical and magneto-optical properties of the films exhibit features which can be determined by the transition of Co^{3+} ions from the low-spin state ($S=0$) to the intermediate-spin state $S=1$. This transition is driven not only by a temperature increase but by an applied magnetic field as well. It is shown as well that the above-indicated properties are dependent on the number of orbital-ordered Co^{3+} ions in a semiconducting matrix. Irrespective of the Sr concentration, the content of the orbital-ordered Co^{3+} ions is the highest at $T\simeq 180$ K. The results obtained support the phase-separation scenario for mixed-valence cobaltites.

ACKNOWLEDGMENT

The authors thank M. A. Korotin for helpful discussions. The study was partially supported by RFBR Grant Nos. 02-02-16429 and 00-02-17797.

*Electronic address: belevtsev@ilt.kharkov.ua

[1] R. von Helmolt, J. Wecker, B. Holzapfel, L. Schultz, and K. Samwer, Phys. Rev. Lett. **71**, 2331 (1993); S. Jin, T.H. Tiffle, M. McCormack, R.A. Fastnacht, R. Ramesh, and L.H. Chen, Science **264**, 413 (1994).

[2] P.M. Raccah and J.B. Goodenough, Phys. Rev. **155**, 932 (1967).

[3] M.A. Korotin, S.Yu. Ezhov, I.V. Solovyev, V.I. Anisimov, D.I. Khomskii, and G.A. Sawatzky, Phys. Rev. B **54**, 5309 (1996).

[4] P. Ravindran, H. Fjellvåg, A. Kjekshus, P. Blaha, K. Schwarz, and J. Luitz, J. Appl. Phys. **91**, 291 (2002).

[5] T. Saitoh, T. Mizokawa, A. Fujimori, M. Abbate, Y. Takeda, and M. Takano, Phys. Rev. B **56**, 1290 (1997).

[6] S. Yamaguchi, Y. Okimoto, and Y. Tokura, Phys. Rev. B **55**, R8666 (1997).

[7] Y. Kobayashi, N. Fujiwara, S. Murata, K. Asai, and H. Yasuoka, Phys. Rev. B **62**, 410 (2000).

[8] C. Zobel, M. Kriener, D. Bruns, J. Baier, M. Grüninger, T. Lorenz, P. Reutler, and A. Revcolevschi, Phys. Rev. B **66**, 020402(R) (2002).

[9] M.A. Señaris-Rodriguez and J.B. Goodenough, J. Solid State Chem. **118**, 323 (1995).

[10] R. Caciuffo, D. Rinaldi, G. Barucca, J. Mira, J. Rivas, M.A. Señaris-Rodriguez, P.G. Radaelli, D. Fiorani, and J.B. Goodenough, Phys. Rev. B **59**, 1068 (1999).

[11] M. Itoh, I. Natori, S. Kubota, and K. Motoya, J. Phys. Soc. Jpn. **63**, 1486 (1994).

[12] P.S. Anil Kumar, P.A. Joy, and S.K. Date, J. Appl. Phys. **83**, 7375 (1998).

[13] J. Mira, J. Rivas, G. Baio, G. Barucca, R. Caciuffo, D. Rinaldi, D. Fiorani, and M.A. Señaris-Rodriguez, J. Appl. Phys. **89**, 5606 (2001).

[14] N.N. Loshkareva, Yu.P. Sukhorukov, E.A. Gan'shina, E.V. Mostovshchikova, R.Yu. Kumaritova, A.S. Moskvin, Yu.D. Panov, O.Yu. Gorbenko, and A.R. Kaul, JETP **92**, 462 (2001).

[15] N.N. Loshkareva, Yu.P. Sukhorukov, E.V. Mostovshchikova, E.V. Nomerovannaya, A.A. Makhnev, S.V. Naumov, E.A. Gan'shina, I.K. Rodin, A.S. Moskvin, and A.M. Balbashev, JETP **94**, 350 (2002).

[16] J. Schoenes, in *Electronic and Magnetic Properties of Metals and Ceramics*, edited by K.H.J. Buschow, Vol. 3A of *Materials Science and Technology* (VCH, Weinheim, 1992), pp. 147–255.

[17] A.K. Zvezdin and V.A. Kotov, *Modern Magnetooptics and Magnetooptical Materials* (IOP, Bristol, 1997).

[18] E.A. Balykina, E.A. Gan'shina, and G.S. Krinchik, Zh. Eksp. Teor. Fiz. **93**, 1879 (1987).

[19] B.I. Belevtsev, N.T. Cherpak, I.N. Chukanova, A.I. Gubin, V.B. Krasovitsky, and A.A. Lavrinovich, J. Phys.: Condens. Matter **14**, 2591 (2002).

[20] B.I. Belevtsev, V.B. Krasovitsky, A.S. Panfilov, and I.N. Chukanova, J. Magn. Magn. Mater. **258–259**, 280 (2003).

[21] M. Ziese, Rep. Prog. Phys. **65**, 143 (2002).

[22] S. Yamaguchi, Y. Okimoto, H. Taniguchi, and Y. Tokura, Phys. Rev. B **53**, R2926 (1996).

[23] N.N. Loshkareva, N.I. Solin, Yu.P. Sukhorukov, N.I. Lobachevskaya, and E.V. Panfilova, Physica B **293**, 390 (2001).

[24] Yu.P. Sukhorukov, N.N. Loshkareva, E.A. Gan'shina, A.R. Kaul, O.Yu. Gorbenko, and K.A. Fatieva, Tech. Phys. Lett. **25**, 551 (1999); Yu.P. Sukhorukov, E.A. Gan'shina, B.I. Belevtsev, N.N. Loshkareva, A.N. Vinogradov, K.D.D. Rathnayaka, A. Parasiris,

and D.G. Naugle, J. Appl. Phys. **91**, 4403 (2002).
[25] T. Arima, Y. Tokura, and J.B. Torrance, Phys. Rev. B **48**, 17 006 (1993).
[26] Y. Tokura, Y. Okimoto, S. Yamaguchi, H. Taniguchi, T. Kimura, and H. Takagi, Phys. Rev. B **58**, R1699 (1998).
[27] S. Yamaguchi, Y. Okimoto, K. Ishibashi, and Y. Tokura, Phys. Rev. B **58**, 6862 (1998).
[28] I. Solovyev, N. Hamada, and K. Terakura, Phys. Rev. B **53**, 7158 (1996).
[29] A.S. Moskvin, E.V. Zenkov, Yu.D. Panov, N.N. Loshkareva, Yu.P. Sukhorukov, and E.V. Mostovshchikova, Fiz. Tverd. Tela (S.-Peterburg) **44**, 1452 (2002).
[30] V. Golovanov, L. Mihaly, and A.R. Moodenbaugh, Phys. Rev. B **53**, 8207 (1996).
[31] R.W. Chantrell, M. El-Hilo, and K. O'Grady, IEEE Trans. Magn. **27**, 3570 (1991).
[32] P. Katiyar, D. Kumar, T.K. Nath, A.V. Kvit, J. Narayan, S. Chattopadhyay, W.M. Gilmore, S. Coleman, C.B. Lee, J. Sankar, and Rajiv K. Singh, Appl. Phys. Lett. **79**, 1327 (2001).
[33] V.G. Bhide, D.S. Rajoria, G.R. Rao, and C.N.R. Rao, Phys. Rev. B **6**, 1021 (1972).
[34] M.A. Señaris-Rodriguez and J.B. Goodenough, J. Solid State Chem. **116**, 224 (1995).
[35] M.R. Ibarra, R. Mahendiran, C. Marquina, B. Garcia-Landa, and J. Blasco, Phys. Rev. B **57**, R3217 (1998).
[36] K. Yoshi, M. Mizumaki, Y. Saitoh, and A. Nakamura, J. Solid State Chem. **152**, 577 (2000).